01

Joule losses in metal-film electrodes with non-uniform surface resistance distribution

© O.A. Emelyanov

Peter the Great Saint-Petersburg Polytechnic University, St. Petersburg, Russia
E-mail: oaemel2@gmail.com

Received March 19, 2025
Revised April 29, 2025
Accepted May 12, 2025

Exact solutions for a number of spatially non-uniform profiles of surface resistance, current and heat flux density distribution of Joule losses in metal-film capacitor structures are considered. The ratio of the total power losses for different profiles indicates a significant (2−3 times) decrease in the total heat release power in the case of using sharply decreasing distributions. The obtained effect is very useful in creating modern metal-film capacitors for efficient capacitive energy storage devices.

Keywords: metal-film capacitor, nanometer thick electrodes, surface resistance, Joule losses.

DOI: 10.61011/TPL.2025.08.61536.20319

The operation of modern metal-film capacitors (MFCs) relies on the well-known self-healing (SH) effect. A significant current density emerges in the case of local breakdown of a dielectric, and the stored energy is dissipated in the breakdown region. This results in partial destruction of a certain circular region of a thin metallized electrode (with a typical thickness of 10−20 nm) near the breakdown channel due to an electrical explosion of the electrode and subsequent microarc discharge. Within several microseconds, a local demetallization zone (several square millimeters in area) forms and isolates the breakdown site from the rest of the electrode, and the capacitor functionality is restored. Thus, MFCs remain operational even at the limit of electrical strength of the polymer dielectric [1]. There are several current trends in development of capacitor technology. One of them is associated with the design of new types of electrode systems for high-voltage film polymer capacitors. Both traditional electrodes with a uniform thickness of Al or Zn metallization and segmented [2] or variable-thickness structures (profiled metallization) [3] are considered. Industrial deposition of non-uniform films has recently been introduced on a pilot scale at several enterprises in Germany, China, and Belgium. The metallization profiles in them are close to the decreasing dependences considered here. In the context of macroscopic effects of Joule losses, the declining trend of the profile and the corresponding comparative calculations are rather more important. The use of profiled metallization with a decreasing nature of square resistance $R_{sq}(x)$ along the electrode allows one to reduce the overall level of Joule losses in MFC electrodes. This is explained qualitatively in Fig. 1, where the top-electrode current is branched off over time via bias current I_D through the dielectric, continues to flow along the bottom electrode, and then returns to the power source.

Thus, the distribution of current I_1 (or its density j) is non-uniform and varies from the initial value I_0 to zero. If one aims to reduce the volumetric heat generation due to Joule losses $q_V(x) = j^2\rho(x)$, it is logical to use low boundary values of surface resistance $R_{sq}(L) = r_L$ in the region of current inflow of a nanometer electrode with thickness d_M and high values of $R_{sq}(0) = r_0$ (resistivity $\rho = R_{sq}d_M$) at the opposite end. It should be taken into account that the specified boundary values are chosen in consideration of several factors.

Modern MFCs use standard polymer dielectric (polypropylene, polyethylene terephthalate) films with a thickness of 3−10 μm onto which metal electrodes (Al or Zn) are deposited using the traditional industrial method of vacuum metallization. The typical thickness of uniform metallization is 5−40 nm (depending on the operational requirements), and the typical surface resistance falls within the range of 5−20 Ω. Such films have a polycrystalline structure with a characteristic grain size on the order of the film thickness. Thinner films have a good capacity for SH, since the energy for evaporation of a local region in the breakdown zone is significantly lower than the one corresponding to relatively thick metallization layers. At the same time, Joule losses in thin films are higher. When the thickness of such electrodes exceeds 40−50 nm (the corresponding resistance is on the order of 0.2−0.5 Ω), a significant amount of released SH energy, which has the capacity to destroy nearby layers of the polymer dielectric, may lead to catastrophic failure. The thickness of reliably produced conductive films on a rough polymer surface with a surface resistance in excess of 50−60 Ω is no lower than 2−3 nm. Low-resistance (several Ω) films with a thickness of more than 40−50 nm are suitable for use in the area of low-resistance contact with external electrodes (heavy edge). However, it is not advisable to raise the thickness further, since thicker films do not allow for efficient self-healing [4]. More in-depth estimates of the relation between the thickness and resistivity of metal films may be found in [5,6] and

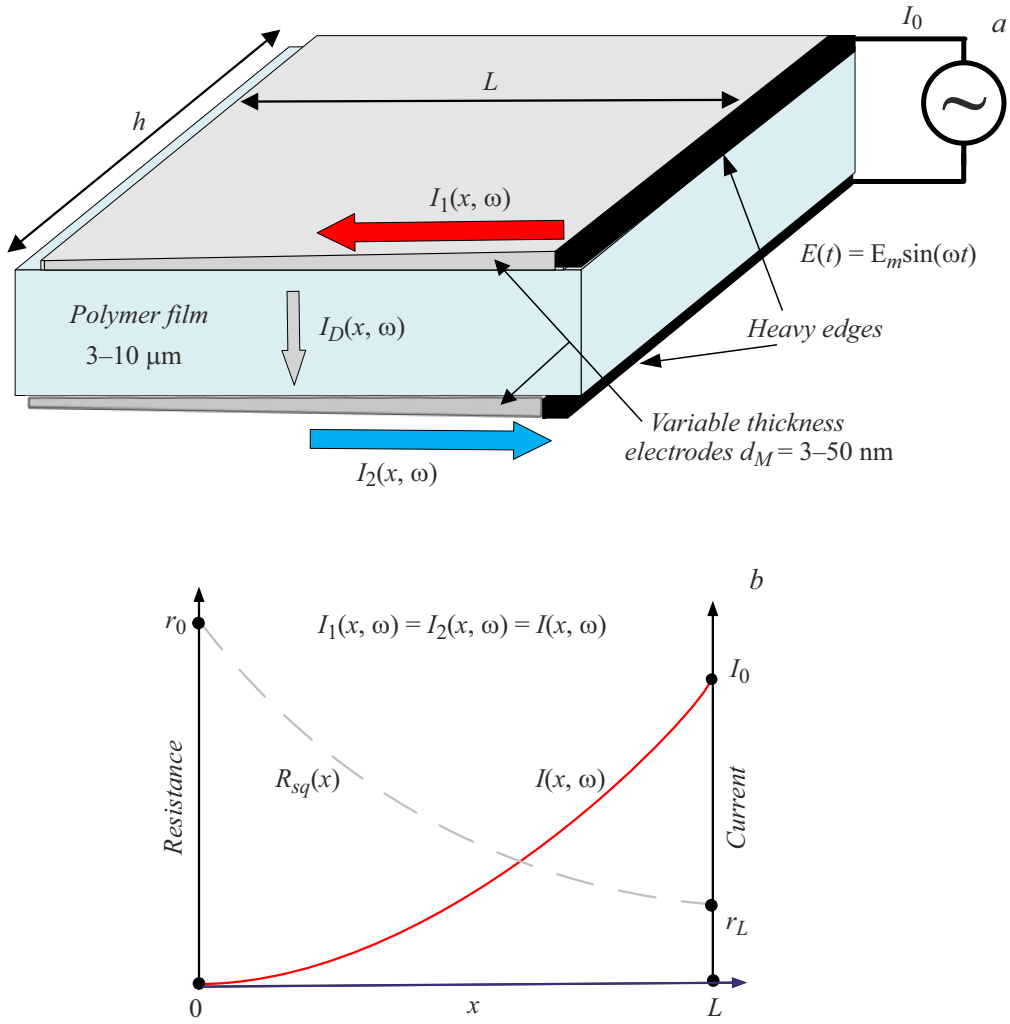

Figure 1. Schematic diagram of the metal-film capacitor structure (a) and distributions of current and resistance of the electrode surface (b).

recent study [7]. At the same time, Joule losses in profiled metallization are usually estimated in the approximation of a linear current distribution along the electrode [8–10], which may introduce a significant error into the calculation results.

In the region of sufficiently high frequencies (from several hundred kilohertz to several megahertz), the introduction of magnetic field into calculations reveals the non-uniformity of current distribution throughout the volume of a capacitor, where phenomena similar to the development of a skin layer in conductors are observed [11]. Additional frequency dispersion of the capacitor capacitance associated with finite parameters of propagation of the electromagnetic field along the capacitor electrode also arises. At high frequencies, the spatial distribution of current deviates from the linear one even if the metallization thickness is uniform [12]. Thus, the electrode–dielectric system should be analyzed with account for the spatial distribution of current and voltage, which becomes very important for calculating the design parameters of capacitors. In real-world scenarios, the problem is reduced to calculating a long line with linear RC elements where the active resistance depends on spatial coordinate x. In most cases, the linear inductance and conductivity may be neglected, since their values are very small. We have proposed a general approach to solving this problem for uniform metallization in [12]; however, the line in the present study is non-uniform. The general solution to the considered problem with arbitrary non-uniformities is unknown. At the same time, exact solutions may be obtained by analyzing specific spatial dependences $R(x)$. The aim of the study was to obtain exact solutions for the spatial current distribution for a number of model dependences $R(x)$. The obtained solutions were used to calculate the total power of Joule losses for different profiles, and conclusions regarding the possible reduction of the total heat release power in the examined cases were made. With this aim in view, we consider the equivalent circuit of a capacitor structure in Fig. 1: a long line with linear capacitance and resistance of electrodes $R(x)$ and C. $E(t)$ is the voltage source for a line of length L. The calculation model of the structure has three regions: a polymer film

with thickness d and permittivity ε and two electrodes with non-uniform metallization resistance $R_{sq}(x)$. The linear parameters for a capacitor with capacitance C_0 may be defined as $R(x) = R_{sq}(x)/h$, $C = C_0/L$, where L is the electrode width, $h = C_0 d/2\varepsilon\varepsilon_0 L$ is the length, and ε_0 is the permittivity of vacuum. The balance of currents and voltages at an arbitrary point with coordinate x of our structure is then reduced to the following system of telegraph equations:

$$\begin{cases} \dfrac{\partial u(x,t)}{\partial x} = 2R(x)i(x,t), \\ \dfrac{\partial i(x,t)}{\partial x} = C\,\dfrac{\partial u(x,t)}{\partial t}, \\ E(t) = u(x,t) + \int\limits_L^x 2R(x)i(x,t)dx, \end{cases} \tag{1}$$

where $u(x,t)$ is the voltage between the electrodes and i is the electrode current. A one-way connection and the symmetrical case with $R1(x) = R2(x) = R(x)$ are considered here. Since the total resistance is the sum of $R1(x) + R2(x) = R(x)$, a factor of 2 arises in the first equation of system (1). Owing to the symmetry of the system, the currents of the top and bottom electrodes have different directions, but are equal in magnitude. Therefore, the Joule losses in the electrodes are the same.

Let us consider the steady-state mode under the influence of a harmonic voltage source $E(t) = E_m \exp(j\omega t)$, where E_m and ω are the amplitude and frequency of the applied voltage. The corresponding complex values of voltage and current are then

$$\begin{cases} \frac{d^2\dot{I}(x,\omega)}{dx^2} = 2j\omega CR(x)\dot{I}(x,\omega), \\ \frac{d^2\dot{U}(x,\omega)}{dx^2} = 2j\omega CR(x)\dot{U}(x,\omega) + \frac{1}{R(x)}\,\dfrac{dR(x)}{dx}\,\dot{U}(x,\omega), \\ \frac{d\dot{I}(x,\omega)}{dx} = 2j\omega C\,\dot{U}(x,\omega), \\ E_m = 2R\int\limits_L^0 \dot{I}(x,\omega)dx + \dot{U}(0,\omega). \end{cases} \tag{2}$$

The boundary conditions for currents and voltages at the start and end of the line are defined as

$$\dot{I}_1(L,\omega) = -\dot{I}_2(L,\omega) = \dot{I}_0,$$

$$\dot{I}_1(0,\omega) = -\dot{I}_2(0,\omega) = 0,$$

$$\dot{U}(0,\omega) = \dot{U}_0,$$

$$\dot{U}(L,\omega) = \dot{E}(t).$$

It is convenient to solve the first equation of system (2) at a given current value I_0 first and then determine the voltage using the third relation. The structure of the equation for current shows clearly that a linear spatial current distribution is feasible only if the second derivative is equal to zero; i. e., the right-hand side must vanish. However, system (2) then becomes entirely meaningless. To obtain correct estimates of the current and voltage distribution, one needs to analyze solutions for specific dependences of the spatial distribution of metallization resistance $R_{sq}(x)$ (or its thickness d_M). Since the typical R_{sq} values for uniform metallization are on the order of 5–20 Ω [4.6], one may take an average value on the order of 10 Ω for quantitative comparison and secure an average value for all metallization profiles at the level of the above-mentioned $r_{mid} = 10\,\Omega$ by varying parameters r_0 and r_L:

$$r_{mid} = \frac{1}{L}\int\limits_0^L R_{sq}(x)dx. \tag{3}$$

Let us turn to the exact solutions for currents, where parameter $k(\omega) = 2\varepsilon\varepsilon_0\omega/d$ is used in all cases.

1. Uniform distribution of metallization resistance $R_{sq}(x) = r_{mid} = r_0 = r_L = 10\,\Omega$:

$$\dot{I}_{mid}(x,\omega) = A\sinh(\alpha(\omega)x),\ \ \alpha(\omega) = \sqrt{ik(\omega)r_{mid}},$$

$$A = \frac{I_0}{\sinh(\alpha(\omega)L)}.$$

2. Linear distribution of metallization resistance ($r_0 = 19\,\Omega$, $r_L = 1\,\Omega$):

$$R_{lin}(x) = ax + b,\ \ \xi(x,\omega) = \frac{k(\omega)(ax+b)}{\sqrt[3]{k(\omega)^2 a^2}},$$

$$\dot{I}_{lin}(x,\omega) = A\left(\mathrm{Bi}\big(\xi(x,\omega)\big) - \mathrm{Ai}\big(\xi(x,\omega)\big)\,\frac{\mathrm{Bi}\big(\xi(0,\omega)\big)}{\mathrm{Ai}\big(\xi(0,\omega)\big)}\right),$$

$$A = \frac{I_0}{\mathrm{Bi}\big(\xi(L,\omega)\big) - \mathrm{Ai}\big(\xi(L,\omega)\big)\,\frac{\mathrm{Bi}\left(\xi(0,\omega)\right)}{\mathrm{Ai}\left(\xi(0,\omega)\right)}}.$$

3. Hyperbolic distribution of metallization resistance ($r_0 = 50\,\Omega$, $r_L = 2\,\Omega$):

$$R_{hyp}(x) = (ax+b)^n,\quad n = -2,$$

$$\alpha(\omega) = \sqrt{1 + 4\,\frac{k(\omega)}{b^2}},\ \ g(x) = \sqrt{ax+b},$$

$$b = r_0^{1/n},\quad a = \frac{1}{L}\,(r_L^{1/n} - r_0^{1/n}),$$

$$\dot{I}_{hyp}(x,\omega) = A(g(x)^\alpha - a^\alpha g(x)^{-\alpha})g(x),$$

$$A = \frac{I_0}{(g(L)^\alpha - a^\alpha g(L)^{-\alpha})g(L)}.$$

4. Exponential distribution of metallization resistance ($r_0 = 55\,\Omega$, $r_L = 4\,\Omega$):

$$R_{exp}(x) = c + b\exp(-\beta x),\ \ \nu(\omega) = \sqrt{\frac{4ck(\omega)}{\beta^2}},\ \ b_m = \frac{b}{\beta^2},$$

$$b = \frac{r_0 - r_L}{1 - \exp(-\beta L)},\quad c = r_0 - b,$$

$$\dot{I}_{exp}(x,\omega) = A1\,J_\nu\big(\nu, 2\sqrt{-k(\omega)b_m}\exp\Big(\frac{-\beta x}{2}\Big)$$

$$- A2\,Y_\nu\Big(\nu, 2\sqrt{-k(\omega)b_m}\exp\Big(\frac{-\beta x}{2}\Big),$$

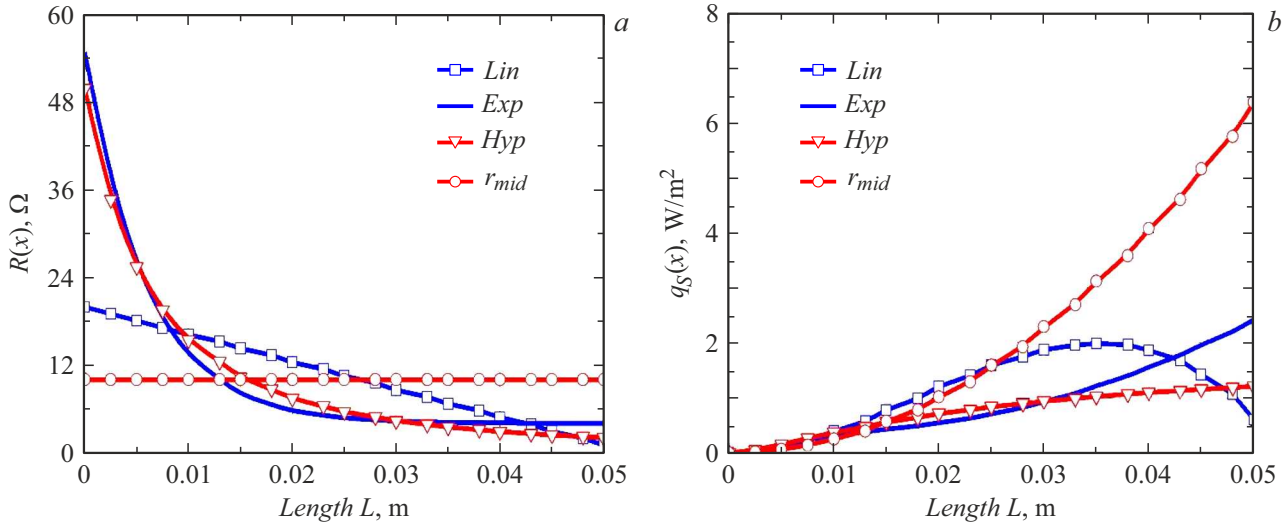

Figure 2. Spatial profiles of metallization resistance $R(x)$ (a) and heat flux density $q_S(x)$ (b) in the electrodes of the capacitor structure.

$$A1 = -A2\,\frac{Y_\nu(\nu, 2\sqrt{-k(\omega)b_m})}{J_\nu(\nu, 2\sqrt{-k(\omega)b_m})},$$

$$A2 = I_0\left[Y_\nu\left(\nu, 2\sqrt{-k(\omega)b_m}\exp\left(\frac{-\beta L}{2}\right)\right)\right.$$

$$\left. - J_\nu\left(\nu, 2\sqrt{-k(\omega)b_m}\exp\left(\frac{-\beta L}{2}\right)\right)\frac{Y_\nu(\nu, 2\sqrt{-k(\omega)b_m})}{J_\nu(\nu, 2\sqrt{-k(\omega)b_m})}\right]^{-1}.$$

$\mathrm{Ai}(x)$ and $\mathrm{Bi}(x)$ in the obtained relations are the Airy functions of the first and second kind, and $J_\nu(x)$ and $Y_\nu(x)$ are the Bessel functions of the first and second kind and order ν, respectively [13].

It is convenient to use the value of local heat flux density $q_S(x)$, which is equal to the product of volumetric heat generation $q_V(x) = j^2\rho(x)$ and metallization layer thickness $d_M(x)$ (j and $\rho(x)$ denote here the current density and the bulk resistivity, and $\rho(x) = R(x)d_M(x)$) for comparative assessment of the distribution of Joule heat generation along the electrode. The flux value itself and the total power of Joule losses P in both electrodes are

$$q_S(x) = q_V(x)d_M(x) = j^2(x)\rho(x)d_M(x)$$

$$= \left(\frac{I(x)}{hd_M}\right)^2 R(x)d_M^2 = \left(\frac{I(x)}{h}\right)^2 R(x),$$

$$P = 2\int_0^L q_S(x)h dx. \qquad (4)$$

Further examples of calculations are performed in accordance with relations (4) for specific values of capacitor capacitance $C_0 = 1\,\mu$F, $L = 5$ cm at $E_m = 320$ V, $I_0 = 2$ A, frequency $f = 1$ kHz, and polypropylene dielectric parameters $d = 5\,\mu$m and $\varepsilon = 2.2$.

Plots of different metallization resistance profiles (a) and heat fluxes $q_S(x)$ (b) are shown for comparison in Fig. 2, where the uneven nature of these dependences is clearly visible. The total loss power is 0.19, 0.23, and 0.3 W for the hyperbolic, exponential, and linear profiles, respectively (for comparison, a constant $r_{mid} = 10\,\Omega$ yields 0.54 W). Thus, the ratio of the total power of Joule losses corresponding to different profiles indicates that sharply decreasing $R(x)$ dependences, such as exponential or hyperbolic ones, provide a significant (2–3-fold) reduction in total heat release power compared to uniform or linearly decreasing profiles. This considerable reduction in total heat release in MFCs may expand significantly the range of permissible operating conditions under high electrical and thermal loads. Intriguingly, the estimated dielectric loss power for the examined polypropylene capacitor is $\omega C_0 E^2 \operatorname{tg}\delta \approx 0.51$ W, which is close to the total Joule loss power in the electrodes at a constant value of $r_{mid} = 10\,\Omega$. An in-depth analysis of dielectric losses in the cases under consideration and the phenomenon of dispersion of the effective capacitance will be performed in future studies.

Funding

This study was supported by the ROSATOM State Atomic Energy Corporation and the Ministry of Science and Higher Education of the Russian Federation as part of federal project 3 (FP3), project No. FSEG-2025-0005.

Conflict of interest

The author declares that he has no conflict of interest.

References

[1] J. Kammermaier, G. Rittmayer, S. Birkle, J. Appl. Phys., **66** (4), 1594 (1989). DOI: 10.1063/1.344373
[2] V.O. Belko, O.A. Emelyanov, J. Appl. Phys., **119**, 024509 (2016). DOI: 10.1063/1.4939954
[3] C. Yi, B. Zhang, C. Li, Q. Li, J. Hu, J. He, IEEE Trans. Dielectr. Electr. Insul., **32** (1), 127 (2025). DOI: 10.1109/TDEI.2024.3403539
[4] V.O. Belko, O.A. Emelyanov, I.O. Ivanov, A.P. Plotnikov, E.G. Feklistov, IEEE Access, **9**, 80945 (2021). DOI: 10.1109/ACCESS.2021.3085695
[5] A.F. Mayadas, M. Shatzkes, Phys. Rev. B, **1** (4), 1382 (1970). DOI: 10.1103/PhysRevB.1.1382
[6] H. Li, Z. Li, F. Lin, H. Jiang, T. Fang, Q. Zhang, IEEE Trans. Plasma Sci., **48** (7), 2523 (2020). DOI: 10.1109/TPS.2020.2998143
[7] M.A. Tarasov, A.A. Lomov, A.M. Chekushkin, A.A. Tatarintsev, B.M. Seredin, M.A. Markina, E.F. Pozdnyakova, A.D. Golovanova, M.V. Strelkov, D.S. Zhogov, R.K. Kozulin, K.Yu. Arutyunov, Tech. Phys. Lett., **51** (2), 97 (2025).].
[8] T. Guan, F. Zhao, T. Fan, X. Wen, IOP Conf. Ser.: Mater. Sci. Eng., **366**, 012031 (2018). DOI: 10.1088/1757-899X/366/1/012031
[9] H. Li, T. In, Y. Fei, H. Li, Z. Li, Power Capacit. React. Power Compens., **36** (5), 37 (2015). DOI: 10.14044/j.1674-1757.pcrpc.2015.05.007
[10] J. Liu, L. Zhu, L. Zheng, S. Ji, in *2021 IEEE Conf. on electrical insulation and dielectric phenomena* (*CEIDP*) (IEEE, 2021), p. 518–521. DOI: 10.1109/CEIDP50766.2021.9705376
[11] C. Joubert, A. Béroual, G. Rojat, J. Appl. Phys., **76** (9), 5288 (1994). DOI: 10.1063/1.357179
[12] O.A. Emelyanov, I.O. Ivanov, Tech. Phys., **63** (1), 111 (2018). DOI: 10.1134/S1063784218010115.
[13] N.N. Lebedev, R.A. Silverman, *Special functions and their applications* (Dover Publ. Inc., 1972).

Translated by D.Safin